

A Scanning Probe Microscopy experimental component designed for early graduate/postgraduates students

J. A. Watson^{1, 2}, S. Myhra³, and G. S. Watson¹,

¹ School of Pharmacy and Molecular Sciences, James Cook University, Townsville, QLD 4811, Australia

² School of Engineering and Physical Sciences, James Cook University, Townsville, QLD 4811, Australia

³ Department of Materials, Oxford University, Begbroke Science Park, Sandy Lane, Yarnton, OX5 1PF, UK

The emergence of courses, subjects and dedicated degree programmes in Nanoscience and Nanotechnology has flourished in recent years with an ever growing number of institutions incorporating such components into their undergraduate and more recently graduate/postgraduate programmes.

An important aspect in relation to the study of Nanoscience and Nanotechnology is the emergence of relatively new instruments/techniques such as Scanning Probe Microscope/y (SPM) and particularly Atomic Force Microscopy (AFM). Indeed most general Materials/Surface Science and associated books will now include mention of SPM or present dedicated chapters on this subject reflecting the current and predicted prominence of this form of microscopy. Here we present a laboratory component incorporating a number of key principles and attributes of the SPM system. These can be easily modified to allow addition of new or different aspects related to SPM or simplification for lower level courses or instrumentation with restricted capabilities. The SPM experimental component has been successfully implemented and refined over a 3 year period.

This experimental component includes the following:

- Hands on operation and familiarity of a Scanning Probe Microscope instrument.
- Fabrication of Micro/Nano structures using SPM lithography (e.g., using a Diamond–Like–Carbon (DLC) film).
- Topographical characterisation of the lithographic outcomes.
- Fabrication of polymeric structures (e.g., Polydimethylsiloxane) based on the lithographic outcomes (moulds) produced.
- AFM characterisation of the fabricated polymer structures in terms of topography, mechanical and adhesive properties and evaluation of the fabrication efficiency from the original lithographic outcomes.

Keywords Scanning Probe Microscopy; Atomic Force Microscopy; Education; Lithography; Nanotechnology; Experiment; Adhesion; Polymer.

1. Introduction

The development of the Atomic Force Microscope (AFM) is arguably one of the most exciting and promising technological breakthroughs to occur in the field of microscopy in recent times as evidenced by the vast number of studies in the literature [e.g., 1-9]. Although having a relatively brief history in comparison with the more traditional forms of microscopy (e.g., Scanning Electron Microscopy (SEM)), AFM has already established itself as a powerful tool in the physical, chemical and more recently the biological sciences. Introducing the AFM to students at both the undergraduate and postgraduate level will not only advance the knowledge base but also encourage students to undertake multi-disciplinary studies for which this instrumentation is perfectly designed for. To this end we had introduced an SPM research based laboratory component into fourth year laboratory courses, exposing physics, engineering and nanoscience students.

Graduate/Postgraduate students require challenging hands on experience commensurate with their academic level. Traditionally laboratories of this nature have a recipe based format with a sequential series of instructions for the students. We have adopted an alternative approach whereby the students are provided with a basic skeletal format introducing basic concepts and listing the experimental tasks required (mirroring real-life experimental problems/plans/tasks). These research based laboratory components incorporate a number of key principles and attributes of the SPM system and can be easily modified to accommodate for different instrument capabilities and in some cases different research or teaching focuses. We present one of three laboratory components which has been formally evaluated and has received the most positive feedback from students interested in Material Science, Surface Science and Nanoscience and Nanotechnology. This research based laboratory has evolved from a 3rd year science degree laboratory where thin films are produced and characterised utilising the AFM – a laboratory which has been running for over 10 years.

The students use (under the guidance and assistance of technical, teaching and/or research staff) the instruments over a two day period in a research laboratory. The involvement of trained operators is necessary in helping the students plan a sequence of experiments to complete the tasks, operate the instruments and also in the transfer of tacit knowledge required during the period. While the use of trained operators (usually research staff) necessitates both a financial and

time commitment, it does provide a teaching framework offering skilled expertise and maximising engagement of the students. Students are also provided with an opportunity and encouraged to ‘play’ with the software and discover its features, potentials and limitations.

Given below is the written information which is provided to the students refined from previous evaluations of the course by students and staff. Material not provided to the students is in *underlined italics* emphasising points of interest, potential problems and general comments.

2. Lab 1

Fabrication of 3- dimensional polymeric nano/micro structures: Characterisation by Atomic Force Microscopy (AFM)

The written information provided to the students is in the form of

- General objectives
- Background information on AFM and general aspects related to the experiments
- A list of the tasks the students will undertake under the guidance of trained staff

Objectives

- Gain hands on operation and familiarity of an atomic force microscope research instrument.
- Fabricate lithographic structures at the micro/nano scales.
- Fabricate polymeric structures from the lithographic outcomes (moulds) produced.
- Characterise the fabricated polymer structures in terms of mechanical and adhesive properties and evaluate the fabrication efficiency from the original lithographic outcomes.

Introduction and Background

The background information for this study will give you a general understanding of the key concepts required for the experiments. Specific tasks will be carried out under the guidance of the SPM research/technical lab staff. Tacit knowledge and additional information from the SPM staff will allow all tasks to be carried out.

Basic operation of the Atomic Force Microscope and measurement of out-of-plane loading forces

The operator sequentially goes through the main points of the lab manual with the students illustrating various concepts/key points.

The Atomic Force Microscope/y (AFM) is based on measurement of forces acting between a sharp tip and a surface [10]. The instrument is basically a 3-dimensional force profiling system. Figure 1 shows a schematic representation of the principal elements of the AFM instrument. A sharp tip is located at the free end of a force sensing element (termed the cantilever or lever). The lever plus the tip is collectively called the ‘probe’. The sample and the tip apex are brought into close proximity while the sharpness of the tip localises the interaction area/volume. The lever provides a simple and effective way to translate the small forces acting between the tip and sample into a measurable quantity. The lever also affords a reflective surface for the optical detection system; an anchorage point for the tip and a resonance frequency higher than the instrumental eigen modes, necessary to minimise unwanted noise. Depending on the stiffness (spring/force constants) of the lever, it may sense tip/sample forces typically in the range from 10^{-6} to 10^{-12} N. The deflection of the lever, and thus the force loading requires monitoring by some form of a detection system.

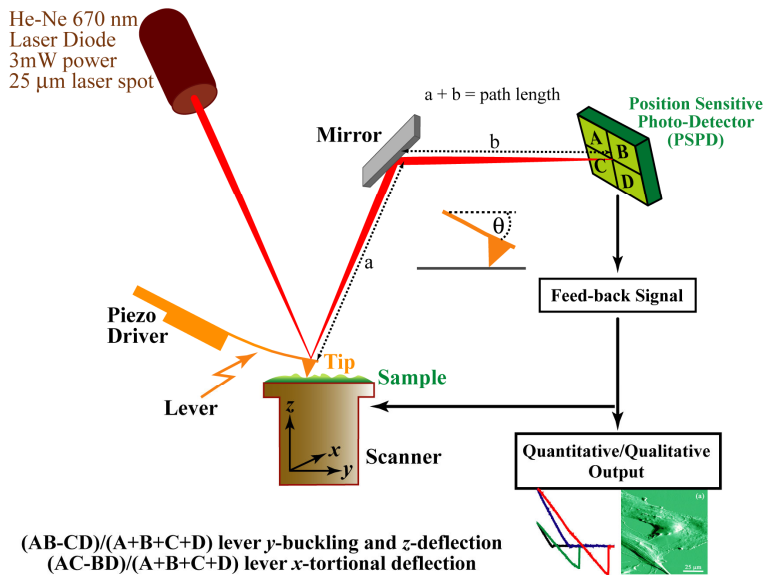


Fig. 1. A schematic showing the principal elements of the Atomic Force Microscope.

The most commonly implemented detection system for commercially available instruments is optical deflection using a laser beam and position sensitive photo-detector (PSPD). The laser beam is reflected off the back of the cantilever (in some instruments the laser beam is directed to the lever by a prism). The reflected beam is then directed via a mirror to the PSPD. The differential signal from the top - bottom and left - right of the detector (using a four-quadrant photodetector) is then used to monitor cantilever angle changes resulting from bending, twisting and buckling of the lever. Thus the lever deflections and spring constants for various directions can be related to the forces required to induce such changes. The force-sensing/imposing probe is shown in Fig. 2.

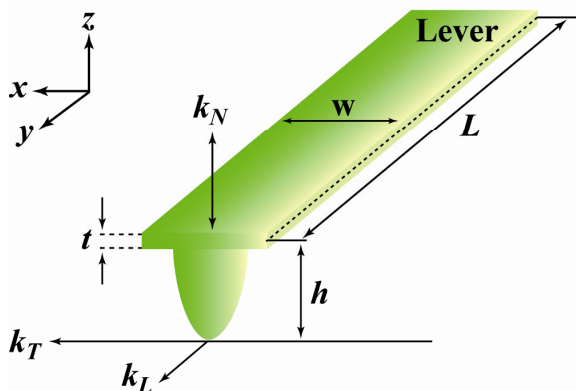


Fig. 2. A schematic representation of a simple beam shaped cantilever with a tip attached at the free end. w , t and L are the width, thickness and length of the beam, respectively, h is the height of the tip, and k_T , k_L and k_N are the torsional, longitudinal and normal spring constants of the lever, respectively.

The three expressions for force/spring constants of deformation - arising from simple bending (k_N), torsion/twisting (k_T) and longitudinal buckling (k_L) - are shown in Eq. 1, 2 and 3, respectively, below [11-13].

$$k_N = \frac{Et^3w}{4L^3} \quad (1)$$

$$k_T = \frac{Gwt^3}{3Lh^2} \quad (2)$$

$$k_L = \frac{k_N L^2}{3h^2} \quad (3)$$

where w = width of lever, L = length of lever, t = thickness, h = height of tip, E = Young's Modulus and G = the shear constant defined by $G = E[2(1-\mu)]^{-1}$ where μ = Poisson's Ratio (ratio of transverse strain to longitudinal strain of the material under stress).

The expressions above (Eq. 1, 2 and 3) assume that the deformation of the lever can be described by the lowest order modes of a long thin beam. In general, when one or more deformational modes are responding to forces acting on the tip, the excursion of its apex along a particular direction is given by

$$\begin{pmatrix} y \\ x \\ z \end{pmatrix} = \begin{pmatrix} \frac{1}{k_L} & 0 & \frac{3h}{2Lk_N} \\ 0 & \frac{1}{k_T} & 0 \\ \frac{L}{2hk_L} & 0 & \frac{1}{k_N} \end{pmatrix} \begin{pmatrix} F_L \\ F_T \\ F_N \end{pmatrix} \quad (4)$$

assuming tip bending, transverse bending of the lever in the x - and z -directions are negligible. Where F_L , F_T and F_N are the longitudinal, torsional and normal force loading, respectively.

A macroscopic model of the lever and the tip (e.g., plastic ruler (lever) with an attached cosmetic sized mirror and plastic funnel (tip)) is useful for explaining the lever motion and deformation states - especially for visually oriented students. A clear demonstration of the relationship between the direction of the travelling tip and the forces acting at the tip apex is easy to demonstrate. Thus out-of-plane (normal loading forces) and in-plane frictional forces can be seen by the translated lever response in terms of bending and twisting. At this point a discussion on what methods can be used to determine the lever spring constant (e.g., manufacturer value, resonance methods, lever on lever [12, 14]) (and thus quantify forces) can be introduced. This is also an ideal time to introduce to the students other modes of operation such as intermittent contact (tapping mode) and non-contact modes. It is also useful to comment on other acronyms and initialisms used for the SPM and explain it is the nature of the interaction which will define this term (e.g., magnetic force microscopy (MFM), etc.

All the science accessible to AFM analysis takes place at the interface between the probe tip and the surface. Accordingly the choice of probe and its mechanical and physico-chemical properties are crucially important. The type of probe selected for imaging will strongly depend on the nature of the information which is desired and the imaging conditions. The surface chemistry of the tip is of critical importance for a number of analyses (e.g., measurement of adhesion, investigation of biomolecular bonding, protein unfolding, analysis of double layer interactions, etc). As well, the surface chemistry will affect friction measurements in the frictional mode of operation. Current probes are commonly microfabricated from Si, SiO₂ or Si₃N₄ using photolithographic techniques (e.g., Albrecht *et al.*, [15]).

A visual inspection of a lever and tip viewed under high optical magnification illustrates the length scales involved.

Generally the AFM is operated in one of the quasi static d-c detection modes (e.g., constant force mode). In its normal mode of operation (contact mode, constant force/constant deflection) the laser spot is essentially kept at the same vertical position on the detector. This is accomplished via a feedback system whereby the sample or tip, which is mounted on an x , y , z -piezoelectric ceramic scanner, is raised or lowered during a raster cycle such that the deflection of the lever remains constant. The z information (z -scanner movements to maintain constant lever deflection) is represented as a brightness factor in the output image.

The macroscopic model of the probe can be used to illustrate the modes of operation.

As the students will need to quantify force loading, adhesion etc., an explanation of the Force-distance mode and force distance curves is required.

Measurement of out-of-plane forces can be carried out using the AFM force-versus-distance (f-d) mode. The AFM f-d mode involves the approach and retract motions of the tip (along the z -direction normal to the sample surface plane) at a fixed location (to a first approximation) in the x - y plane. This will measure interactions near the interface and at the surface of the sample.

Figure 3 shows a representative f-d curve on a 'hard' surface in air, where compression at the point of contact can be neglected. The horizontal axis of the f-d curve represents the position of the sample/scanner-stage along the z -direction. The vertical axis represents the force exerted on the tip along the z -direction and is measured by monitoring the top and bottom segments of the photo-detector. The f-d curve is broken up into an approach and retract curve and a number of points (A-G) reflecting the tip-sample distance and interaction along the z -direction. These points are described in greater detail below in the figure caption. The hysteresis created between the approaching and retracting probe is a consequence of frictional forces acting between the tip and surface, scanner artefacts and the irreversibility of various interactions, e.g., meniscus forces.

Once again a macroscopic model of the probe can be used to identify the various points in figure 3.

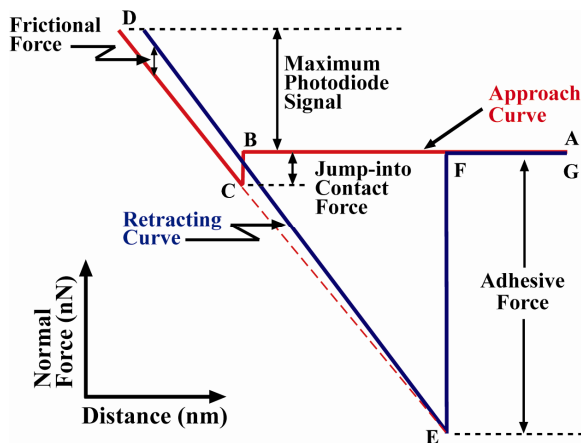


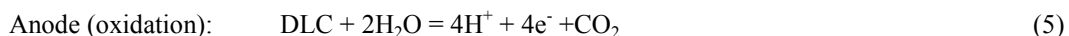
Fig. 3. Representative f-d curve on a surface (e.g., mica/silicon) in air. In this case the sample is a ‘hard’ surface and thus suitable for calibrative purposes. The net force (deflection of the lever) is sensed during the approach, contact and retract parts of the cycle. The forces along the z-direction (F_N) can be calculated by $k_N\Delta z$ – where Δz is the z-axis deflection of the lever. Region A-B describes the sample and probe as being not in contact, but approaching with minimal forces acting at this stage. B-C shows the motion of the lever as it is brought close to the sample. The tip senses attractive forces (generally from a meniscus layer in air) which cause the lever to bend downward. The attractive force gradient exceeds the spring constant of the lever, and this instability causes the tip to snap into contact with the surface. C-D shows the response of the sensor which measures cantilever/tip displacement. The tip and surface are incompressible, and the stage travel distance must therefore be equal to the lever deflection. The cantilever continues to bend, being the only compliant element, so that extent of lever bending is precisely equal to stage travel. This part of the curve is used to measure and calibrate force loadings. D-E shows the tip beginning to retract from the surface. Adhesion between the tip and sample maintains the contact. The meniscus interaction has increased due to capillary action, and there will be a greater lift-off instability/discontinuity (than for the snap-on). E-F describes the jump of the cantilever away from surface, when the mechanical lever retraction force becomes greater than the adhesive forces.

AFM Manipulation/Lithography of surfaces

The AFM can be used to manipulate a variety of surfaces (irreversibly in many cases) by utilising a number of different approaches [16-18]. For example, the lever implied force can be used to mechanically remove material from a surface such as a polymer to create pre-determined surface structures and/or patterns [e.g., 19, 20]. One alternative to applying a lever imposed force for lithography is to create chemical and/or physical changes on a surface by applying a potential difference between the tip and surface [e.g., 21]. This is accomplished by utilising a tip-to-surface bias, with the tip being effectively a travelling electrode. For instance, oxide structures with line-width resolution better than 10 nm can be written by an SPM probe to a silicon surface or certain metallic substrates by “anodic” oxidation, e.g., [22-25]; and oxidative nano-lithographic patterning of amorphous graphitic carbon films and of electrically conducting diamond-like carbon (DLC) films has been described [26-28].

Diamond-Like-Carbon (DLC) is a generic term for a class of materials able to be synthesized by a variety of well-established routes, leading to phases that are diamond-like, with hardness and other mechanical properties being also comparable to those of crystalline diamond. DLC is now finding increasing industrial usage, for example coatings for video tapes and hard drive discs, coating on razor blades and high temperature electronics just to name a few.

The likely respective reactions of lithographically altered DLC using AFM can be written as:



The overall reaction can be written as



Two examples of lithographically altered DLC are shown in Figs. 4 and 5 below.

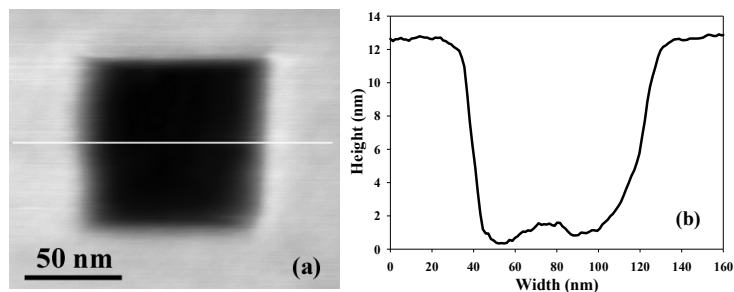


Fig. 4. Contact mode image (a), and cross-sectional contour line (c) illustrate a square pit formed as a result of carrying out tip-induced spatially resolved oxidation on a DLC surface.

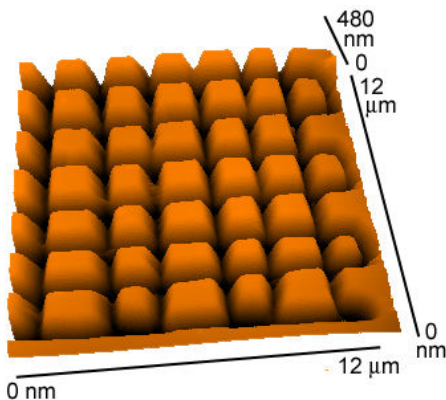


Fig. 5. AFM image (3-D representation) of a DLC patterned surface created with a tip bias. Lithographic software was used for regulating the position and speed of the mobile tip.

Not all AFM instrumentation has the facility for electrochemically tip induced alteration. In this case the SPM operated in the STM mode can be used to fabricate the structures. (Note: the manipulation of DLC carried out here is in air (not liquid) although high humid conditions are favourable). Alternatively, there are many sources of micro/nano templates in the literature (e.g., natural nanostructures) which can be utilized as a template for making polymer structures. An example is shown in the figure 6 below where a commercially available patterned surface on a silicon wafer was used (a), with the polymer PDMS replica obtained from the patterned surface (b). In this case the AFM images were taken at the extremities of the scanning areas to illustrate non-linearities of the piezoelectric elements.

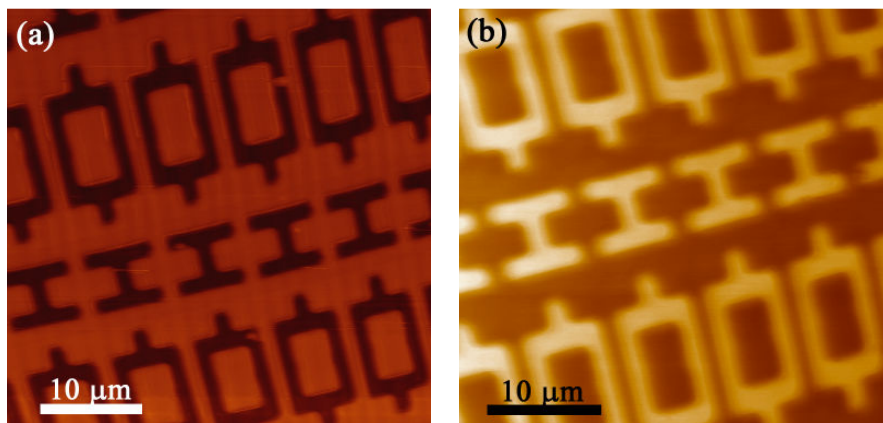


Fig. 6. AFM images of a patterned silicon wafer (a) and a PDMS replica (b).

Polymeric Micro/Nano structures

Micron sized structures/components are commonly employed in a variety of devices (e.g., biosensors, array devices). At present such devices are predominantly based on macro/microscopic technologies e.g., photolithography. Future applications of differentiated structures/surfaces are expected to place considerable demands on down-sizing technologies. Thus, patterning of surfaces at smaller length scales is becoming increasingly important for micro/nano fabrication. An emerging set of methods known collectively as soft lithography is now being utilised for a large variety of applications including micromolding, microfluidic networks and microcontact printing [29]. In particular, stamps and elastomeric elements can be formed by exposure of a polymer to a template. The 'template' can be fabricated by a

variety of techniques capable of producing well-defined surface topographies. Established lithographic techniques used in the microelectronic industry, such as photolithography, are generally used to fabricate such master templates at the micron scale. In this experiment you will fabricate templates on the micro/nano scale using Diamond–Like–Carbon (DLC) films (as discussed in the previous section).

A number of different polymers can be moulded for use as micro/nano stamps. One of the most widely used polymers for these purposes is polydimethylsiloxane (PDMS). The molecular structure of 5 repeat units of a siloxane bond is shown in Fig. 7. Table 1 shows some of the physical properties of the PDMS polymer.

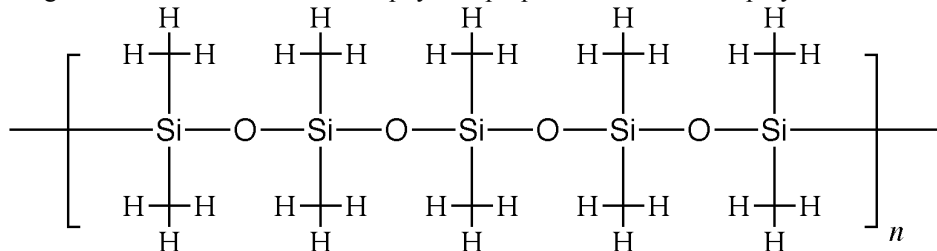


Fig. 7. Molecular structure of 5 repeat units of a siloxane bond.

Table 1 – PDMS properties

Property	Characteristics
Physical	
Appearance	Transparent, optical detection 240 – 1100 nm [29, 30]
Young's Modulus	Tunable, typically \sim 750 kPa [31, 32]
Thermal Conductivity	0.2 W/(m·K) [30]
Coefficient of thermal expansion	310 $\mu\text{m}/(\text{m} \cdot ^\circ\text{C})$ [30]
Surface Free Energy	Low; \sim 20 erg.cm $^{-2}$ [33]
Electrical	
Breakdown voltage	$2 \times 10^7 \text{ Vm}^{-1}$ [30]

The PDMS elastomer is chemically resistant, has a low surface energy and readily conforms to different surface topographies. Obtaining a template is generally considered the limiting factor in the production of PDMS replicas. An example of a PDMS replica (showing a ‘negative’ pattern of the original structuring) using DLC as the master pattern is shown in Fig. 8 (a) and (b).

The use of DLC allows the students to design individual patterns for replication. Abstract designs, pictures or letters/words are all easily implemented with most AFM software lithographic packages.

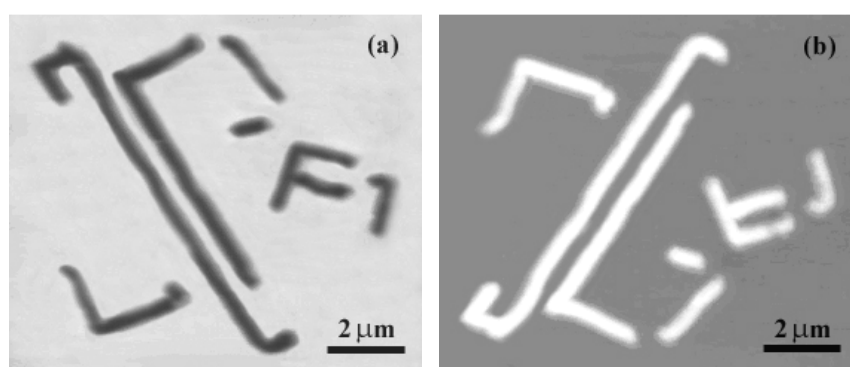


Fig. 8. Topographical images of a DLC template (a), and the resultant PDMS stamp (b).

The PDMS polymer is relatively inexpensive and easily made by the mixing of curing and base agents. Once a thin coat has been applied to the master pattern it can be left to cure overnight (1 day is sufficient at ambient temperatures or a few hours at 60–80°C). Removing the polymer is relatively easy and requires simply peeling the coating off with tweezers, starting at one edge. The amount of PDMS placed on the master needs to be in a sufficient quantity that the polymer holds together as one piece when removed. This is generally a good place to end day 1 of the experiment.

Determining Surface Mechanical Properties

In order to determine the surface properties associated with elastic deformation of the tip and the sample, a model based on continuum mechanics is usually adopted. The various models have different strengths and weaknesses for different experimental situations. The choice of model is particularly important whenever a load dependence is required. Classical continuum mechanics is usually justifiable since even small indentations of the tip and sample will lead to contact area of many tens of atoms.

A lever-induced force will cause deformation at the tip-to-surface interface. If the tip is taken to be incompressible, then the deformation is confined to the sample. The depth of indentation (σ) as a function of applied force (F_N) will depend on the shape of the tip and on the mechanical properties of the surface. For sample deformations using a rigid tip, a number of expressions are available depending on the tip geometry [34].

For a conical tip, the applied force (F_{cone}) as a function of sample indentation (σ) is described by

$$F_{cone}(\sigma) = \frac{2E^*}{\pi \tan \alpha} \sigma^2 \quad (8)$$

where α is the conical half (AFM) tip angle and E^* is the relative Young's modulus, defined as:

$$\frac{1}{E^*} = \frac{1 - \mu_{tip}^2}{E_{tip}} + \frac{1 - \mu_{sample}^2}{E_{sample}} \quad \left(\approx \frac{1 - \mu^2}{E_{sample}} \text{ for } E_{tip} \ll E_{sample} \right) \quad (9)$$

The force F_{par} for a parabolic tip is given by

$$F_{par}(\sigma) = \frac{4\sqrt{R}}{3} E^* \sigma^{1.5} \quad (10)$$

where R is the tip radius of curvature. The elastic deformation of the sample due to a rigid sphere can be expressed as:

$$\sigma = \frac{1}{2} \eta \ln \left(\frac{R + \eta}{R - \eta} \right) \quad (11)$$

where η is the contact radius. The relationship between the loading force and the contact radius will be:

$$F_{sphere} = \frac{E^*}{2} \left[(\eta^2 + R^2) \ln \left(\frac{R + \eta}{R - \eta} \right) - 2\eta R \right] \quad (12)$$

The Bilodeau model [35] describes the indentation of an elastic half-space by a regular n -sided pyramidal probe; a standard Si₃N₄ probe tip, to a very high degree of accuracy. When $n = 4$, the Bilodeau model predicts the following relationship (Eq. 13) between force, F , and depth of indentation, σ , from which Young's modulus, E , can be obtained.

$$F_{Pyramid} = \frac{3E \tan \alpha}{4(1-\nu^2)} \sigma^2 \quad (13)$$

where α is the opening half-angle of the pyramid (55° for a 'standard' Si₃N₄ tip), and μ is in the range 0.3-0.5.

Finally the indentation equation considering the tip as a flat-ended cylinder is given by:

$$F_{cylinder} = 2RE^* \sigma \quad (14)$$

It is possible to estimate the indentation on a material at a particular applied force by aligning the force curves for a hard and soft surface so that the contact points coincide (see Fig. 9). The error (ΔCp) associated with such measurements primarily arises from the determination of the contact point on the soft surface. If the sample is soft in relation to the sensitivity of the lever, then the uncertainty in the contact point can lead to significant errors in calculation of indentation depth, Young's modulus, or any other parameter defined by the contact point. The sensitivity of the AFM in this context requires close matching of the lever spring constant, k_N , to the elastic constant of the sample surface. If the lever spring constant is too high then the sample will deform significantly before the lever deflects measurably. This condition may result in the derivative of the force curve near the point of contact being undetectable from the non-contact part of the curve.

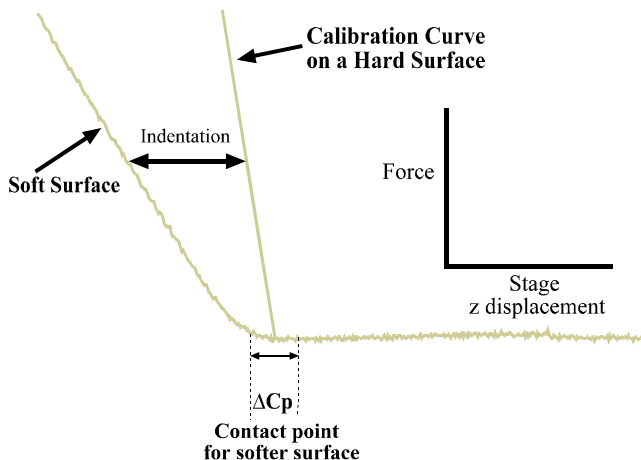


Fig. 9. Diagram showing indentation determination by alignment of the contact points for a hard and soft surface. The error (ΔC_p) in the contact point for the soft surface is also shown.

A number of questions/points are raised in this section:

The importance of the choice of the spring/force constant for the PDMS polymer. PDMS is a relatively soft polymer and will deform under light loads.

What assumptions are based in the equations? The contact equations assume deformations arising from perfectly flat elastic substrates that adopt the shape of the tip profile. Plastic deformations and surface roughness influences are not considered. PDMS under high loads can be plastically deformed [17]. Also, the equations do not take into account the surface energies of the two surfaces. Adhesion is considered in the contact mechanics theories of Derjaguin, Müller and Toporov (DMT) [36], and Johnson, Kendall and Roberts (JKR) [37]. For simplicity we suggest that the students use the DMT model to calculate the total force loading. In this way they simply add the adhesive force to the applied loading.

The experiment also allows the students to base their calculated values using the most appropriate theory of interaction. It is useful for the students to plot a graph of $\ln(F_N)$ versus $\ln(\sigma)$ with the indentation equations as this will determine the contact geometry and thus the appropriate equation used to calculate the material contact properties (e.g., Young's Modulus). PDMS will generally conform to the tip shape.

It is useful to comment on how the AFM produces force images which, in common with other microscopic techniques, suffer from a variety of artefacts (see Table 2) which must be taken into account in order to interpret the data fully and reliably. Any such artefacts or noise observed on the students' images are encouraged to be discussed in their report.

Table 2. AFM associated artefacts.

Piezoelectric Ceramics Scanner	Probe/Lever/Tip	Other
non-linearity	radius of curvature	vibrational noise
hysteresis	aspect ratio/opening angle	thermal changes
creep	tip asymmetry	feedback control
aging effects of ceramic	tip flexing/bending	data manipulation
z-range limit	contamination	sample softness
	tip shape e.g. double tip	sample movement
	probe/sample angle	charging effects
		probe/sample forces

Tip convolution is a critical point here and an important concept for the student to appreciate, particularly when the students evaluate the efficiency of the pattern transfer from the DLC surface to the polymer surface. Ideally tip characterisation should be carried out in situ, using the AFM itself as the imaging tool. This procedure is possible on samples used in the experiment which have a well defined structure (e.g., natural nanostructures, sharp edges etc).

The experiment can be taken to the next obvious step where the students use the polymeric structures as stamping elements. The stamps can be inked with an appropriate chemistry (e.g., thiols) and stamped onto a surface (e.g., Au, Silicon). Evaluation of the second transfer process (stamping) can be explored by optical microscopy or by AFM to examine topography and/or friction. It is relatively easy to incorporate research that is currently of interest in the scientific community into this experimental framework. For example, other tribological properties such as friction can be integrated within the lab. DLC has a low coefficient of friction and it is easy for the students to measure this value

and compare it to other materials of interest. Partly coating a small piece of DLC with PDMS and then examining the edge location shows a dramatic example of frictional contrast on materials.

Tasks

The AFM operator will guide the students through the following tasks. Generally most tasks can be handled by the students. Probe placement and sometimes detector alignment may need to be shown.

- Use AFM lithography to create a template on the DLC surface.
- Obtain Topographical images of the master/template surface.
- Use the template to fabricate a PDMS surface incorporating the replica features.
- Obtain a Topographical image of the PDMS surface and determine the efficiency of the molding process.
- Determine the adhesion force between the tip and the surface by obtaining a sufficient amount of f-d curves. An error analysis (e.g., Standard Deviation) must also be included.
- Calculate the mechanical micro/nano stiffness (Young's Modulus) of the polymer surface.
- Compare this value with macroscopic measurements (Table 1).

3. Conclusion

The information, framework and acquired skills obtained by the students in this laboratory component reflect some of the key attributes of the scanning probe and atomic force microscope. These include topographical imaging of surfaces, manipulation of surfaces using probe techniques, measurements of force using force-distance curves (applied loading, adhesion etc.), and application of this data to determine surface mechanical properties. Other important concepts are also introduced such as, tip convolution, applicability of contact models and AFM artefacts. Components of soft-lithography are also introduced. The material presented as a AFM component can be easily modified to introduce other SPM capabilities such as frictional measurements.

References

- [1] Ratner M, Ratner D. Nanotechnology: A Gentle Introduction to the Next Big Idea. New Jersey, USA; Prentice Hall PTR; 2003.
- [2] Meyer E, Overney RM, Dransfeld K, Gyalog T. Nanoscience: Friction and Theology on the Nanometer Scale. Singapore World Scientific Publishing Co. Pte. Ltd.; 1998.
- [3] Nalwa HS, ed. Encyclopedia of Nanoscience and Nanotechnology. California, USA; American Scientific Publishers; 2004.
- [4] Goddard WA, Brenner DW, Lyshevski SE, Iafrate GJ, eds. Handbook of Nanoscience, Engineering, and Technology. USA; CRC Press LLC; 2003.
- [5] Mansoori GA. Principles of Nanotechnology: Molecular-Based Study of Condensed Matter in Small Systems. Singapore; World Scientific Publishing Co. Pte. Ltd.; 2005.
- [6] Kolasinski KW. Surface Science: Foundation of Catalysis and Nanoscience. England; John Wiley & Sons, 2002.
- [7] Roco MC, Bainbridge WS, eds. Societal Implications of Nanoscience and Nanotechnology. The Netherlands; Kluwer Academic Publishers; 2001.
- [8] Crandall BC. Nanotechnology: Molecular Speculations on Global Abundance. USA; Massachusetts Institute of Technology; 1996.
- [9] Schulz MJ, Kelkar AD, Sundaresan MJ, eds. Nanoengineering of Structural, Functional, and Smart Materials. USA; CRC Press LLC; 2006.
- [10] Binnig G, Quate CF, Gerber C. Atomic Force Microscopy. *Physics Review Letters*. 1986;56:930-933.
- [11] Warmack RJ, Zheng X-Y, Thundat T, Allison DP. Friction effects in the deflection of atomic force microscope cantilevers. *Review of Scientific Instruments*. 1994;65:394-399.
- [12] Gibson CT, Watson GS, Myhra S. Scanning Force Microscopy - Calibrative procedures for 'Best Practice'. *Scanning*. 1997;19:564-581.
- [13] Ogletree DF, Carpick RW, Salmeron M. Calibration of frictional forces in Atomic Force Microscopy. *Review of Scientific Instruments*. 1996;67:3298-3306.
- [14] Cleveland JP, Manne S, Bocek D, Hansma PK. A non-destructive method for determining the spring constant of cantilevers for Scanning Force Microscopy. *Review of Scientific Instruments*. 1993;64:403-405.
- [15] Albrecht TR, Akamine S, Carver TE, Quate CF. Fabrication of microcantilever stylus for the atomic force microscope. *J. Vac. Sci. Technol. B*. 1990;8:3386-3389.
- [16] Bushell GR, Watson GS, Holt SA, Myhra S. Imaging and nano-dissection of tobacco mosaic virus by atomic force microscopy. *J. Microsc.* 1995;180:174-181.
- [17] Watson JA, Brown CL, Myhra S, Watson GS. Two-dimensional stick-slip on a soft elastic polymer: Pattern generation using atomic force microscopy. *Nanotechnology*. 2006;17:2581-2589.
- [18] Watson GS, Myhra S, Cribb BW, Watson JA. Putative function(s) and functional efficiency of ordered cuticular nano-arrays on insect wings. *Biophys. J.* 2008;94:3352-3360.

- [19] Blach JA, Watson GS, Brown CL, Pham DK, Wright J, Nicolau DV, Myhra S. A mechanistic approach to tip-induced nanolithography of polymer surfaces. *Thin Solid Films*. 2004;459:95-99.
- [20] Cappella B, Sturm H, Weidner SM. Breaking polymer chains by dynamic plowing lithography. *Polymer*. 2002;43:4461-4466.
- [21] Myhra S, Watson GS. Tip-induced nano-writing/machining of Si and DLC surfaces – “anodic” versus thermal oxidation? *Appl. Phys. A*. 2005;81:487-493.
- [22] Avouris P, Hertel T, Martel R. Atomic force microscope tip-induced local oxidation of silicon: Kinetics, mechanism, and nanofabrication. *Appl. Phys. Letts.* 1997;71:285-287.
- [23] Myhra S. Bias-induced spatially resolved growth and removal of Si-oxide by atomic force microscopy. *Appl. Phys. A*. 2003;76:63-69.
- [24] Vullers RJM, Ahlskog M, van Haesendonck C. Field induced local oxidation of Ti and Ti/Au structures by an atomic force microscope with diamond coated tips. *J. Vac. Sci. Technol. B*. 1999;17:2417-2422.
- [25] Mühl T, Brückl H, Weise G, Reiss G. Nanometer-scale lithography in thin carbon layers using electric field assisted scanning force microscopy. *J. Appl. Phys.* 1997;82:5255-5258.
- [26] Mühl T, Brückl H, Kraut D, Kretz J, Mönch I, Reiss G. Nanolithography of metal films using scanning force microscope patterned carbon masks. *J. Vac. Sci. Technol. B*. 1998;16:3879-3882.
- [27] Mühl T, Kretz J, Mönch I, Schneider CM. Parallel nanolithography in carbon layers with conductive imprint stamps. *Appl. Phys. Letts.* 2000;76:786-788.
- [28] Myhra S. Tip-induced oxidative nano-machining of conducting diamond-like carbon (DLC). *Appl. Phys. A*. 2005;80:1097-1104.
- [29] McDonald JC, Whitesides GM. Poly(dimethylsiloxane) as a material for fabrication microfluidic devices. *Accounts of Chemical Research*. 2002;35:491-499.
- [30] Dow Corning Corp., Sylgard-184, Midland, MI, <http://www.dowcorning.com>.
- [31] Armani D, Liu C, Aluru N. Re-configurable fluid circuits by PDMS elastomer micromachining, *12th International Conference on MEMS, MEMS 99*, 222-227, Orlando, Florida; 1998.
- [32] Unger MA, Chou J-P, Thorsen T, Scherer A, Quake SR. Monolithic microfabricated valves and pumps by multilayer soft lithography. *Science*. 2000;288:113-116.
- [33] Chaudhury MK, Whitesides GM. Direct measurements of interfacial interactions between semispherical lenses and flat sheets of Poly(dimethylsiloxane) and their chemical derivatives. *Langmuir*. 1991;7:1013-1025.
- [34] Sneddon N. The relation between load and penetration in the axisymmetric boussinesq problem for a punch of arbitrary profile. *International Journal of Engineering Science*. 1965;3:47-57.
- [35] Bilodeau G. Regular pyramid punch problem. *Journal of Applied Mechanics*. 1992;59:519-523.
- [36] Derjaguin BV, Muller VM, Toporov YP. Effect of contact deformation on the adhesion of particles. *Journal of Colloid Interface Science*. 1975;53:314-326.
- [37] Johnson KL, Kendall K, Roberts AD. Surface energy and the contact of elastic solids. *Proc. of the Royal Society of London, A (Mathematical and Physical Sciences)*. 1971;324(1558):301-313.